AEROSOL SCIENCE AND TECHNOLOGY
2017, VOL. 51, NO. 3, 388–396
http://dx.doi.org/10.1080/02786826.2016.1263384

Taylor & Francis
Taylor & Francis Group

Rebounding hygroscopic inorganic aerosol particles: Liquids, gels, and hydrates

Y.-J. Li[a,b], P.-F. Liu[a], C. Bergoend[a], A. P. Bateman[a], and S. T. Martin[a]

[a]John A. Paulson School of Engineering and Applied Sciences & Department of Earth and Planetary Sciences, Harvard University, Cambridge, Massachusetts, USA; [b]Department of Civil and Environmental Engineering, Faculty of Science and Technology, University of Macau, Macau

ABSTRACT

Particle rebound was studied for ten atmospherically relevant inorganics. Experiments were conducted with submicron particles in aerosol form to a relative humidity (RH) of <5% followed by progressive exposure to RH up to 95% for 2 s. At low RH, particles of $MgCl_2$, NaCl, NH_4Cl, KCl, $(NH_4)_2SO_4$, and Na_2SO_4 crystallized. As RH increased, these particles completed the transition from rebounding to adhering close to their deliquescence RH (DRH). The onset of decreased rebound, however, was below the DRH. Rebound curves for particles of $MgCl_2$, NH_4NO_3, $MgSO_4$, and $NaNO_3$ had different features than explained by water adsorption and deliquescence. Particles of $MgCl_2$ had rebound curves characterized by two domains, corresponding to its two hydrates. At low RH, particles of $MgSO_4$ and $NaNO_3$ did not crystallize but rebound occurred, suggesting a glassy or high-viscosity though noncrystalline state. Gel formation for $MgSO_4$ can increase viscosity, affecting rebound behavior. Particles of NH_4NO_3 adhered even to <5% RH, suggesting a low-viscosity state even to low RH. Particles of NH_4HSO_4 were investigated as a special case by exposure to 5 ppm ammonia at 10% and 90% RH. At low RH, these particles still had sufficient molecular diffusivity to maintain active heterogeneous chemistry, although with some kinetic limitations. The different behaviors between nitrates and sulfates suggest different roles of heterogeneous chemistry in regions affected by NO_x compared to SO_2 emissions. The results of this study could have implications for the use of different wet and dry seed particles in chamber experiments.

ARTICLE HISTORY
Received 10 September 2016
Accepted 12 November 2016

EDITOR
Kihong Park

1. Introduction

Atmospheric aerosol particles affect global climate (IPCC 2013), visibility (Hyslop 2009), and human health (Poschl 2005). Physicochemical properties of aerosol particles can govern the extent of these effects when they occur. For example, diameter changes associated with the hygroscopic growth of aerosol particles increase their efficiency for light attenuation (Zieger et al. 2015). Size changes also alter the penetration of aerosol particles into the human respiratory tract (Londahl et al. 2007). Hygroscopic water uptake can change the viscosity and thus the phase states of atmospheric aerosol particles by lowering the average molecule weight with water acting as a plasticizer (Koop et al. 2011). The liquid, semi-solid, or solid physical state of aerosol particles can affect species diffusion within the interior of the particle (Kuwata and Martin 2012; Li et al. 2015). Species diffusion can be an important factor in other gas-particle interactions, including evaporation and condensation (Shiraiwa et al. 2012) as well as heterogeneous oxidation (Shiraiwa et al. 2010; Liu et al. 2016).

Particle rebound has been used in recent years to study the physical state of atmospheric particles, especially those largely dominated by organic composition (Virtanen et al. 2010; Bateman et al. 2016). A systematic analysis of the effects of physical state on particle rebound of inorganic particles, however, remains to be done. Inorganic ions such as sulfate, nitrate, ammonia, sodium, potassium, and magnesium are major components responsible for water uptake by aerosol particles (Martin 2000). The dependence of hygroscopic growth on relative humidity (RH) for inorganic particles has been a long-term interest to atmospheric research community, with implications for visibility- and climate-related optical properties (e.g., scattering) of atmospheric particles. For hygroscopicity, in mixed particles the Raoult effect of most inorganic salts dominates over that of organic species in respect to water uptake (Varutbangkul et al. 2006; Smith et al. 2011).

CONTACT Y.-J. Li yongjieli@umac.mo Department of Civil and Environmental Engineering, E11, Faculty of Science and Technology, University of Macau, Macau, Taipa, Macao; S. T. Martin scot_martin@harvard.edu School of Engineering and Applied Sciences, Department of Earth and Planetary Sciences, Harvard University, Harvard Engineering & Applied Sciences, Pierce Hall 122, 29 Oxford St, Cambridge, MA 02138, USA.
Supplemental data for this article can be accessed on the publisher's website.

Unlike mixed organic species, many inorganic salts can adopt a crystalline state at sufficiently low RH. The phase transitions between solid and liquid states follow a hysteresis cycle between deliquescence and efflorescence. This behavior differs from the gradual water uptake and release for amorphous organic materials. Pure salt particles typically remain solid below the deliquescence RH (DRH) during humidification and abruptly transition into liquid above the DRH. A sharp transition in rebound might be expected. A complication, however, is that the inorganic materials can take up water on the surface. As a result, a water meniscus can form between the particle and the impaction plate, and the attractive forces associated with this meniscus decrease particle rebound even before a phase transition, as shown for ammonium sulfate (Bateman et al. 2014). Thus, rebound can be a complicated phenomenon, and systematic laboratory studies are motivated to understand the possible processes.

Herein, experimental results are presented for the rebound of ten inorganic salts as a function of RH from <5% to 95%. The selected salts have a frequent occurrence in atmospheric aerosol particles. The results are analyzed in the context of the hygroscopic influence on the prevalence of liquids, gels, and hydrates. In an additional set of studies, NH_4HSO_4 was exposed to 5 ppm ammonia at 10% and 90% RH for 370 s, and possible effects on rebound were studied.

2. Experimental

Aerosol particles of ten different inorganic salts (Table 1) were generated by an atomizer (TSI, model 3076, TSI Inc., Shoreview, MN, USA). Aqueous solutions of inorganic salts were prepared using Nanopure water (18.1 MΩ cm) for mass concentrations ranging from 0.005 to 0.025% (w/w) in the atomizer reservoir. After passing through a diffusion dryer (<5% RH) at 293 ± 2 K, the particles were size selected in a differential mobility analyzer (DMA, TSI Inc., model 3085, 10:1 sheath-to-sample flow). The mobility diameter was set to 300 nm.

The rebound apparatus was described in detail previously (Bateman et al. 2014, 2015, 2016). The apparatus is represented in Figure S1. Briefly, after size selection in the DMA, particles were passed first through a Nafion-tube setup to control RH and then through one of three single-stage impactors operated in parallel. Impactor 1 (null arm) had no impaction plate after the nozzles, thereby passing all particles downstream less any incidental losses, such as diffusive wall loss. Impactor 2 (capture arm) had an impactor plate coated with vacuum grease, thereby eliminating particle rebound and passing no particles downstream except for non-impacting particles. Impactor 3 (rebound arm) had an uncoated impactor plate, thereby passing rebounded particles downstream. Particle number concentrations downstream of each impactor were recorded by three condensation particle counters (CPC, TSI, model 3010, 1 Lpm). The capture and rebound arms had cut-point diameters of 277.7 ± 3.3 nm for the experiments herein. The particle number concentrations measured downstream of the three arms were denoted as N_1, N_2, and N_3 for null, capture, and rebound arms, respectively, and the rebound fraction f was calculated as follows (Bateman et al. 2014):

$$f = \frac{N_3 - N_2}{N_1 - N_2} \quad [1]$$

The behavior of sucrose particles was used as a reference to characterize the transition in physical properties between adhering and rebounding particles (Bateman et al. 2015). The RH value (i.e., water activity times 100 for sufficiently large particles) at which sucrose particles transitioned from completely rebounding to completely adhering particles occurred across a viscosity range of 10^2 to 10^0 Pa s. This change in viscosity was coincident with a change from a liquid defined as having a viscosity of 10^2 Pa s (Koop et al. 2011).

As a special additional study, aerosol particles of partially neutralized ammonium hydrogen sulfate (NH_4HSO_4) were exposed to ammonia (5 ppm for 370 s) at 10% and 90% RH. The exposure followed the method of Li et al. (2015). After ammonia exposure, the particles were dried through a silica gel diffusion drier and then directed to the three-arm impaction apparatus, and RH-dependent rebound curves were collected.

3. Results and discussion

The efflorescence RH (ERH) and DRH from literature of the ten inorganic salts of this study are summarized in Table 1. The DRH values are consistent among different studies, as expected for this thermodynamic property. $MgCl_2$ has two common hydrates, each with its own DRH value (Schindelholz et al. 2014). In regard to kinetic properties, most salts effloresce 30% to 50% below their respective DRH values. Three salts, however, do not effloresce as aerosol particles even to low RH, including NH_4NO_3, $NaNO_3$, and $MgSO_4$. There is some controversy in the literature surrounding the ERH of NH_4HSO_4, and a separate series of experiments based on NH_3 exposure was designed.

The rebound curves collected in this study for these ten salts are shown in Figure 1. Reproducibility from duplicate experiments is shown in Figure S2 with the data included in the SI. Datasets of rebound curves from

Table 1. Summary of efflorescence RH (ERH) and deliquescence RH (DRH) from literature.

Inorganic Salt	ERH (%)	DRH (%)	Reference	TRH_f(%)[h] (this study)
NH_4NO_3	n/a[a]	62	(Tang 1996)	n/a[a]
	25–32	60	(Dougle et al. 1998)	
	n/a[a]	61.8 ± 0.3	(Lightstone et al. 2000)	
	n/a[a]	62	(Lee and Hsu 2000)	
$NaNO_3$	32	74.3	(Richardson and Snyder 1994)	13
	n/a[a]	74.5	(Tang and Munkelwitz 1994)	
	0.05–30	70	(Lamb et al. 1996)	
	40	71–73	(Liu et al. 2008)	
	n/a[a]	74.0 ± 0.5	(Gupta et al. 2015b)	
$MgCl_2$	<1.5[b]	12–15 or 33[c]	(Schindelholz et al. 2014)	13
	6.8–7.2[d]	15.9 ± 0.3[d]	(Gupta et al. 2015a)	
	9.1–10.8[e]	33[e]	(Gupta et al. 2015a)	
$MgSO_4$	n/a[a]	86[f]	(Ha and Chan 1999)	60
	n/a[a]	92[f]	(Apelblat and Manzurola 2003)	
NH_4HSO_4	0.05–22	40	(Tang and Munkelwitz 1994)	43
	<2	39	(Cziczo et al. 1997)	
	16 ± 2.5[g]	66–76	(Colberg et al. 2004)	
	n/a[a]	40–45	(Schlenker et al. 2004)	
$(NH_4)_2SO_4$	48	80.6–81.3	(Cohen et al. 1987a,b)	79
	37–40	80	(Tang and Munkelwitz 1994)	
	33 ± 2	79 ± 1	(Cziczo et al. 1997)	
	33	75	(Liu et al. 2008)	
	37.9 ± 0.5	79.9 ± 0.3	(Ahn et al. 2010)	
NaCl	44	74–76	(Cohen et al. 1987a,b)	75
	45.5	75.3	(Richardson and Snyder 1994)	
	43 ± 2	75 ± 1	(Cziczo et al. 1997)	
	47	76	(Lee and Hsu 2000)	
	48	75	(Liu et al. 2008)	
	47.7 ± 0.5	75.5 ± 0.2	(Ahn et al. 2010)	
	47.4 ± 0.5	75.6 ± 0.3	(Li et al. 2014)	
	49–51	76–77	(Schindelholz et al. 2014)	
	45.7–47.6	75.1 ± 0.5	(Gupta et al. 2015a)	
NH_4Cl	45	76.5–77.3	(Cziczo et al. 1997)	76
KCl	59	83–86	(Cohen et al. 1987a,b)	78
	56 ± 1	85 ± 1	(Freney et al. 2009)	
	58.7 ± 0.7	84.6 ± 0.3	(Ahn et al. 2010)	
	57.7 ± 0.5	84.7 ± 0.2	(Li et al. 2014)	
	59–61	88	(Schindelholz et al. 2014)	
Na_2SO_4	55	85.4–86.5	(Cohen et al. 1987a,b)	84
	57–59	84	(Tang 1996)	
	58.5 ± 0.6	84.4 ± 0.3	(Ahn et al. 2010)	

Also listed is the observed RH at which the rebound fraction dropped by 90% (TRH_f).
[a]Not available.
[b]Incomplete loss of water even at RH < 1.5% (Schindelholz et al. 2014).
[c]Deliquescence of hexahydrate $MgCl_2 \cdot 6H_2O$ at 33% RH and possibly other hydrates at 12 to 15% RH.
[d]For $MgCl_2 \cdot 4H_2O$.
[e]For $MgCl_2 \cdot 6H_2O$.
[f]RH above saturated salt solution.
[g]Crystal was suggested to be in the form of $(NH_4)_3H(SO_4)_2$ (letovicite); data were for experiments at 260–270 K.
[h]The RH value at rebound fraction of 10% of the maximum rebound fraction from the fitted curve described by Equation (2).

duplicate experiments were fit using a modified sigmoidal equation (Figure 1) (Bateman et al. 2014):

$$f = f_{\max} + A\left(1 + \exp\left(\frac{\mathrm{RH}_{50} - \mathrm{RH}}{\xi}\right)\right)^{-1} \quad [2]$$

where $f_{\max}$ is the maximum rebound fraction, A is a fitted parameter, RH_{50} is the RH value at 50% of $f_{\max}$, and ξ is the width parameter of the sigmoid. Smaller ξ represents a sharper sigmoid. Width is alternatively expressed as the transition RH (TRH) range, representing the 10% onset (TRH_i) and 90% completion (TRH_f) of the transition in rebound fraction. Parameter values, including TRH ranges, are listed in Table 2 for the fits to the rebound curves of each salt.

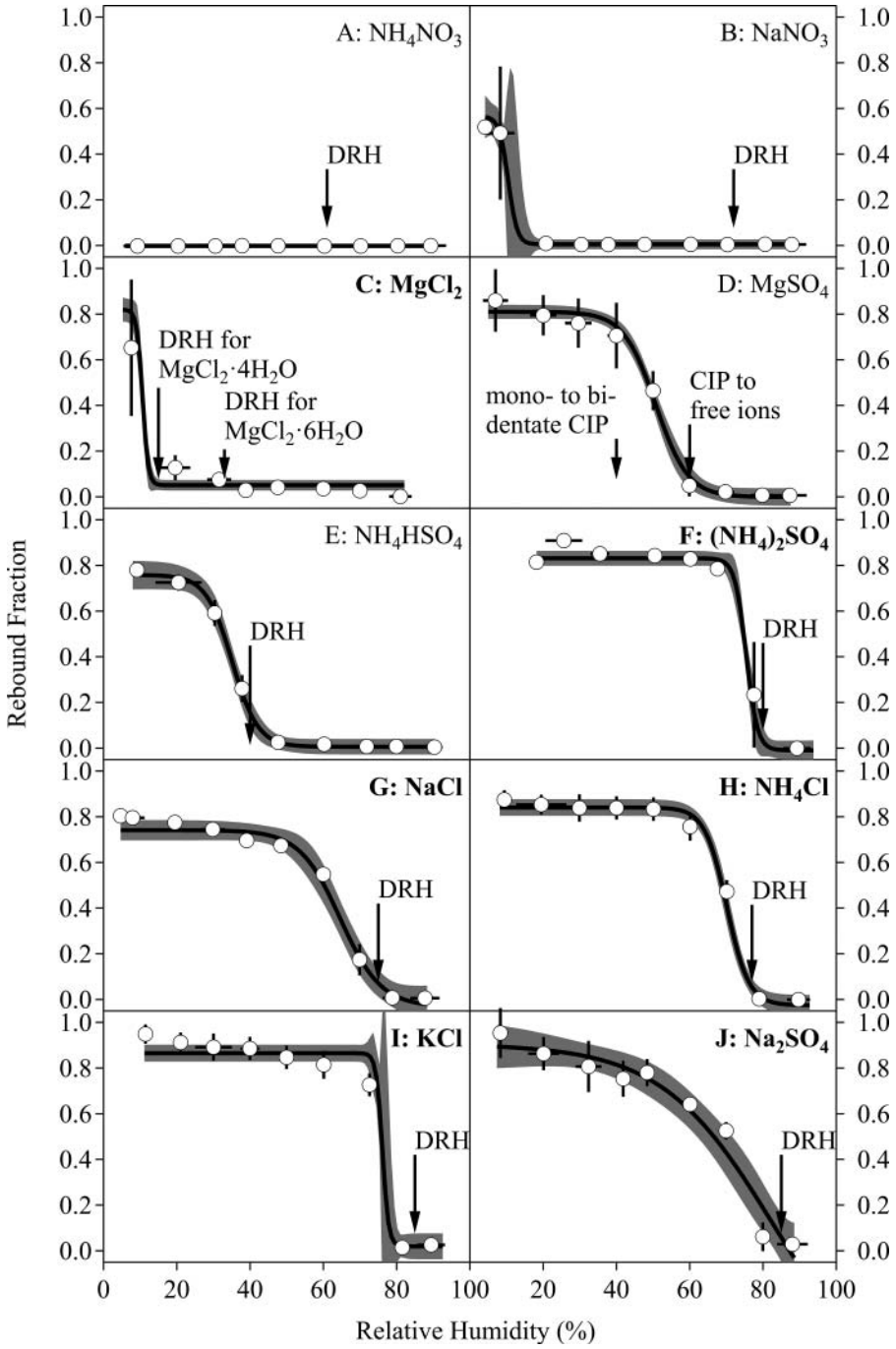

Figure 1. Rebound fraction for aerosol particles of ten inorganic salts: (a) ammonium nitrate, (b) sodium nitrate, (c) magnesium chloride, (d) magnesium sulfate, (e) ammonium hydrogen sulfate, (f) ammonium sulfate, (g) sodium chloride, (h) ammonium chloride, (i) potassium chloride, and (j) sodium sulfate. Bold labeling indicates that the materials became crystalline solid when conditioned at low RH (Martin 2000). Uncertainty bars represent propagated uncertainties for multiple data points in binned RH ranges from duplicate experiments. The black line represents fitting to the data set based on Equation (2). The arrows indicate the DRH values from the literature. The shaded region represents uncertainty based on fitting of all the data points from duplicate experiments (Figure S2). Particles were pre-conditioned to <5% RH prior to the rebound measurements at higher RH.

The fitted curves, including 95% confidence interval ranges in gray shading, appear as thick black lines in Figure 1. In some cases, the fit lines pass close to but not through all the data points. Equation (2) accounts for the broad features of an impactor but does not include the detailed physics of rebound between the particle and the impactor, which can include, for example, attractive forces of formation of a meniscus of water. Its formulation also

Table 2. Summary of fitted parameters for the rebound curves of the ten salts using Equation (2).

Inorganic Salt	f_{max}[a]	RH_{50} (%)[b]	ξ[c]	TRH_f–TRH_i (%)[d]
NH_4NO_3	n/a[e]	n/a[e]	n/a[e]	n/a[e]
$NaNO_3$	0.57 ± 0.11	10 ± 3.5	1.2 ± 3.1	8–13
$MgCl_2$	0.82 ± 0.06	11 ± 0.4	0.8 ± 0.5	9–13
$MgSO_4$	0.81 ± 0.03	51 ± 1.4	4.4 ± 1.2	41–60
NH_4HSO_4	0.76 ± 0.06	35 ± 1.5	3.5 ± 1.3	27–43
$(NH_4)_2SO_4$	0.83 ± 0.03	75 ± 0.6	1.5 ± 0.9	72–79
NaCl	0.74 ± 0.04	65 ± 3.0	5.5 ± 2.5	52–75
NH_4Cl	0.84 ± 0.04	70 ± 1.2	3.0[f]	63–76
KCl	0.86 ± 0.04	76 ± 2.5	0.8 ± 1.7	74–78
Na_2SO_4	0.90 ± 0.13	83 ± 44	15.2 ± 15.4	42–84

[a]Maximum rebound fraction from the fitted curve.
[b]The RH value at rebound fraction of 50% from the fitted curve.
[c]Parameter of quantifying sigmoid steepness.
[d]Transition RH (TRH), defined as the RH range with $0.1f_{max}$–$0.9f_{max}$.
[e]Not available.
[f]Fixed ξ for fitting.

does not account for complex particle behavior, such as the formation of different forms of hydrates and gels. These aspects are discussed further below for applicable salts.

The data sets of Figure 1 show that aerosol particles of nine of the studied salts transitioned from rebounding to adhering as RH increased from <5% to >95%. Particles of NH_4NO_3 were the exception, which did not rebound even to <5% RH, suggesting that they remained liquid even to low RH. Particles of $NaNO_3$ and $MgSO_4$ rebounded for <15% and <60% RH, respectively. These transitions were significantly below the known DRH values (Table 1), suggesting that these particles did not form crystalline solids even to low RH, at least for submicron particles studied herein in aerosol form studied for exposure timescales of seconds (Martin 2000). In respect to the other salts, particles of $MgCl_2$ completed a transition to liquid particles by 35% RH (cf. discussion below about hydrates). Particles of NH_4HSO_4, KCl, NaCl, NH_4Cl, $(NH_4)_2SO_4$, and Na_2SO_4 transitioned to liquids for 40% ± 2%, 78 ± 2%, 75% ± 2%, 76 ± 2% RH, 79 ± 2% RH, and 84 ± 2% RH, respectively.

For the salts $NaNO_3$ and $MgSO_4$ that did not effloresce even to low RH yet did rebound, the observations imply that these salts became highly viscous at sufficiently low RH. A hypothesis is that glasses or rigid gels might form, thus possibly explaining the absence of efflorescence yet the observation of particle rebound. A glass transition temperature close to room temperature has been inferred for anhydrous $NaNO_3$ (Dette and Koop 2015). For $MgSO_4$, gel formation for <40% RH is documented (Chan et al. 2000; Wang et al. 2005; Zhao et al. 2006). The gel arises from chains of hydrated contact-ion pairs. Water diffusion in $MgSO_4$ particles at RH <40% is slow (Cai et al. 2015; Davies and Wilson 2016). Above 40% RH, bidentate contact-ion pairs break and monodentate contact-ion pairs start to form, and rates of water diffusion correspondingly increase. Above 60% RH, free hydrated ions of sulfate and magnesium prevail (Wang et al. 2005). The observations in Figure 1d show no rebound above 60% RH, implying a fully liquid state and thus consistent with the studies on the RH-dependent evolution of the contact-ion pairs. For 40% to 60% RH, rebound increased gradually, which again was consistent with the evolution of effective molecular weight and viscosity as contact-ion pairs progressively decreased and the gel dissipated.

In regard to the salts undergoing deliquescence, this process for pure materials occurs at a singular RH value as governed by Gibbs phase rule of thermodynamics. In most instruments deliquescence therefore manifests itself as a sharp transition consistent with heterogeneities or reproducibility in RH. The measurement uncertainty corresponds to the technique itself (e.g., aerosol flow tube infrared spectroscopy [AFT-IR; Zhao et al. 2006], electrodynamic balance [EDB; Chan et al. 2000], or hygroscopic tandem differential mobility analyzer [HTDMA; Biskos et al. 2006]). The narrowest TRH ranges observed herein (e.g., KCl) lie within this same category of technique uncertainty (Table 2). By comparison, broader TRH ranges (e.g., NaCl) are also observed and in these cases they are indicative of additional phenomena other than deliquescence which affect rebound.

In some cases, the difference between the RH of onset compared to that of final adherence can be explained by a water meniscus at impact that decreases particle rebound even before a phase transition. For RH < DRH, mass and size growth can occur because a thin film or meniscus of water forms on the surface of the solid particles. These changes are often too small for detection by AFT-IR, EDB, or HTDMA, although careful experiments can reveal them. For example, Dai et al. (1995) show water adsorption on the surface of NaCl by infrared observations. Romakkaniemi et al. (2001) and Biskos et al. (2006) studied NaCl nanoparticles and measured

diameter changes by HTDMA. For the rebound measurement, adhesion can occur because of the forces associated with a meniscus neck formed between particle and impaction surface. For instance, non-hygroscopic, non-deliquescent particles of polystyrene latex (PSL) had a rebound fraction of 0.4 at 95% RH because of the role of surface water that affects rebound (Bateman et al. 2014). In the current study, rebound curves of $(NH_4)_2SO_4$ (Figure 1f), NH_4Cl (Figure 1h), and KCl (Figure 1i) particles are representative of this effect. The broader rebound curves of NaCl (Figure 1g) and Na_2SO_4 (Figure 1j) particles can also be explained by this effect, implying that these two salts take up even greater amounts of adsorbed water below DRH. The results of Romakkaniemi et al. (2001) show the greater adsorption of water by NaCl compared to $(NH_4)_2SO_4$ particles. Furthermore, the first monolayer of water on NaCl is complete at 38–40% RH (Peters and Ewing 1997; Luna et al. 1998; Kendall and Martin 2005), which is consistent with TRH_i for the rebound curve of NaCl (Figure 1g).

For crystallizing particles, the formation and deliquescence of metastable salts can also broaden rebound curves, as compared to single-salt deliquescence. For particles of $MgCl_2$, a stepwise change in rebound fraction is evident (Figure 1c). The metastable hydrate $MgCl_2{\cdot}4H_2O$ has a transition at 15% RH to the stable hydrate $MgCl_2{\cdot}6H_2O$, which in turn has a DRH of 33% RH (Gough et al. 2014, 2015a; Schindelholz et al. 2014). Figure 1c shows that the rebound fraction for $MgCl_2$ has stepwise changes across this RH range. There could be an externally mixed population of $MgCl_2{\cdot}6H_2O$ and metastable aqueous particles between 15% and 33% RH, depending on the individual stochastic fates of $MgCl_2{\cdot}4H_2O$ above 15% RH (i.e., transition to hexahydrate in some cases and deliquescence in other cases). These processes broaden the rebound curve.

For the particles of NH_4HSO_4, the interpretation of the RH-dependent rebound experiments is ambiguous. On the one hand, the rebound transition is consistent with the DRH value, thereby suggesting efflorescence at low RH followed by deliquescence on increasing RH. On the other hand, many experimental results show the absence of efflorescence for submicron particles of NH_4HSO_4 exposed to low RH for several minutes at room temperature (Cziczo et al. 1997; Martin et al. 2003; Schlenker et al. 2004; Rosenoern et al. 2008; Mifflin et al. 2009). Based on these studies, the interpretation of the rebound results is that particles of NH_4HSO_4 do not crystallize but become highly viscous at low RH. Other studies suggest that supermicron NH_4HSO_4 particles observed for sufficiently long time periods or lower temperatures can effloresce (Tang and Munkelwitz 1994; Colberg et al. 2003). Given the ambiguity from the RH-dependent rebound experiments alone, additional experiments were carried out for NH_4HSO_4 particles.

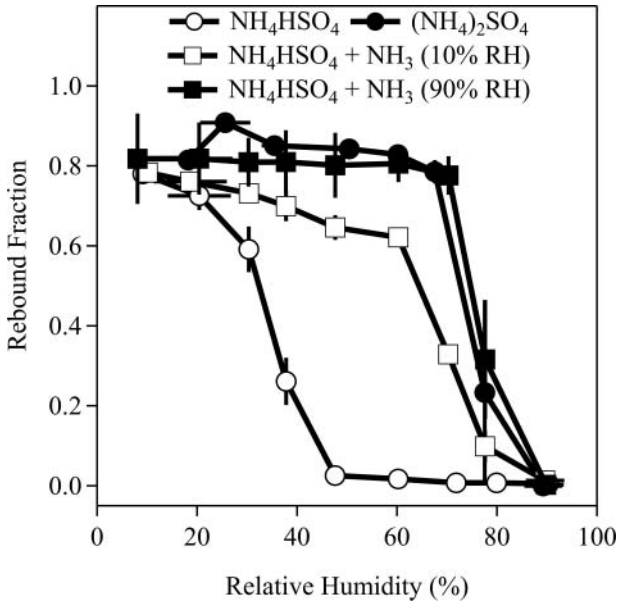

Figure 2. Effect of ammonia exposure on the rebound curves of particles initially composed of aqueous ammonium hydrogen sulfate. Rebound curves are shown after exposure to ammonia at 10% or 90% RH, followed in both cases by conditioning to <10% RH prior to collected of the RH-dependent rebound curves.

NH_4HSO_4 particles were exposed to NH_3 (5 ppm) at low (10%) and high (90%) RH conditions, followed in both cases by conditioning to <10% RH prior to collection of the RH-dependent rebound curves. The resulting rebound curves are shown in Figure 2, together with those of unexposed NH_4HSO_4 particles and reference $(NH_4)_2SO_4$ particles. For exposure at high RH (90%), complete neutralization of aqueous NH_4HSO_4 to $(NH_4)_2SO_4$ was observed, as indicated by the correspondence in the experimental rebound curve with that of the reference. By comparison, for the exposure at low RH (10%), the particles had rebound curves intermediate to those of NH_4HSO_4 and $(NH_4)_2SO_4$ particles, suggesting incomplete neutralization for exposure to 5 ppm NH_3 for 370 s. One possible explanation is that the diffusivity of NH_3 in NH_4HSO_4 particles at 10% RH is low enough that there is a kinetic limitation to NH_3 uptake (Li et al. 2015). An alternative explanation is that initial NH_3 uptake is associated with the production of a crystalline layer of $(NH_4)_2SO_4$ that inhibits further uptake. Another possible alternative explanation is that sufficient neutralization occurred such that $(NH_4)_3H(SO_4)_2$ (letovicite) crystallized (Martin 2000), and further NH_3 uptake did not take place. This salt has a DRH of 69% (Tang and Munkelwitz 1994; Martin 2000), which is coincident with the RH range of sharp change in Figure 2. Although the collected data sets cannot distinguish among these

possibilities, they do suggest that the particles of NH_4HSO_4 were in a viscous rather than an effloresced crystalline state at low RH. The data also demonstrate that unexpectedly small amounts of NH_3 can be taken up by NH_4HSO_4 (i.e., incomplete neutralization in a nominally NH_3-rich environment), which could have implications for the modeling of environmental processes in environments with low RH and possibly low temperature (e.g., free troposphere).

4. Conclusions and atmospheric implications

The final relative humidity for the transition from rebounding to adhering particles, indicative of the transition from liquid to non-liquid particles, agreed with the respective deliquescence relative humidity for six of the ten salts. These salts had in common that they effloresced at sufficiently low RH to form crystalline solids. For other salts, the rebound curves indicate that submicron particles of $NaNO_3$ and $MgSO_4$ adopted a glassy or high-viscosity though non-crystalline state at low RH. Particles of NH_4NO_3 adhered even to low RH, suggesting that they maintained a low viscosity and implying a liquid state. The rebound experiments in conjunction with the ammonia uptake experiments suggest that particles of NH_4HSO_4 also become viscous semisolid at low RH, at least for submicron particles at room temperature across time periods of 2 s.

NH_4NO_3, along with NH_4HSO_4 and $(NH_4)_2SO_4$, can be considered as the most atmospherically relevant of the different studied salts based on frequency of atmospheric occurrence, and the relative importance of NH_4NO_3 is growing given current worldwide emissions trends in NH_3, NO_x, and SO_2(Bauer et al. 2007). An implication is that the inorganic portion of the atmospheric aerosol in polluted environments might increasingly favor liquid over solid states in the next few decades, thus possibly further facilitating mass transfer and reactive chemistry between the gas and particle phases. Ammonium-nitrate-rich particles in the atmosphere at low to intermediate RH may facilitate molecular diffusion and heterogeneous chemistry within the interior of the particles in ways that ammonium-sulfate-rich particles have not.

Inorganic salt particles are often used in studies of secondary organic aerosol (SOA) to provide an initial surface area concentration for the condensation of low-volatility organic species (Kokkola et al. 2014; Zhang et al. 2015; Nah et al. 2016). Many studies have employed crystalline $(NH_4)_2SO_4$ particles and have assumed absorptive partitioning governs the gas-to-particle condensation (Pankow 1994; Donahue et al. 2006). By comparison, the sulfate and nitrate salts that frequently dominate the inorganic composition of the atmospheric aerosol are often aqueous for the prevailing RH, especially near forested environments which provide important precursors to SOA production. The miscibility and possible reactive uptake into these aqueous particles can be integral to SOA production and particle mass yield (Wong et al. 2015), and these processes can be missed in traditional chamber studies that use crystalline particles. Wang et al. (2015) further showed that aqueous NaCl and $NaNO_3$ particles at high RH can enhance the uptake of organic acids by the substitution and release of HCl and HNO_3 to the gas phase. In this light, the results of the present study concerning the liquid, gel, and hydrate states of ten salts as a function of relative humidity provides important information for the design and interpretation of SOA chamber experiments.

Funding

This research was supported by the Office of Science of the Department of Energy and the National Science Foundation. Y.-J. Li gratefully acknowledges the support from the Start-up Research Grant (SRG2015-00052-FST) of the University of Macau.

References

Ahn, K. H., Kim, S. M., Jung, H. J., Lee, M. J., Eom, H. J., Maskey, S., and Ro, C. U. (2010). Combined use of Optical and Electron Microscopic Techniques for the Measurement of Hygroscopic Property, Chemical Composition, and Morphology of Individual Aerosol Particles. *Anal. Chem.*, 82:7999–8009.

Apelblat, A., and Manzurola, E. (2003). Solubilities and Vapour Pressures of Saturated Aqueous Solutions of Sodium Tetraborate, Sodium Carbonate, and Magnesium Sulfate and Freezing-Temperature Lowerings of Sodium Tetraborate and Sodium Carbonate Solutions. *J. Chem. Thermodyn.*, 35:221–238.

Bateman, A. P., Belassein, H., and Martin, S. T. (2014). Impactor Apparatus for the Study of Particle Rebound: Relative Humidity and Capillary Forces. *Aerosol Sci. Technol.*, 48:42–52.

Bateman, A. P., Bertram, A. K., and Martin, S. T. (2015). Hygroscopic Influence on the Semisolid-to-Liquid Transition of Secondary Organic Materials. *J. Phys. Chem. A*, 119:4386–4395.

Bateman, A. P., Gong, Z. H., Liu, P. F., Sato, B., Cirino, G., Zhang, Y., Artaxo, P., Bertram, A. K., Manzi, A. O., Rizzo, L. V., Souza, R. A. F., Zaveri, R. A., and Martin, S. T. (2016). Sub-Micrometre Particulate Matter is Primarily in Liquid form Over Amazon Rainforest. *Nat. Geosci.*, 9:34–37.

Bauer, S. E., Koch, D., Unger, N., Metzger, S. M., Shindell, D. T., and Streets, D. G. (2007). Nitrate Aerosols Today and in 2030: A Global Simulation Including Aerosols and Tropospheric Ozone. *Atmos. Chem. Phys.*, 7:5043–5059.

Biskos, G., Russell, L. M., Buseck, P. R., and Martin, S. T. (2006). Nanosize Effect on the Hygroscopic Growth Factor of Aerosol Particles. *Geophys. Res. Lett.*, 33:L07801, doi:10.7810.01029/02005GL025199.

Cai, C., Tan, S. H., Chen, H. N., Ma, J. B., Wang, Y., Reid, J. P., and Zhang, Y. H. (2015). Slow Water Transport in $MgSO_4$Aerosol Droplets at Gel-Forming Relative Humidities. *Phys. Chem. Chem. Phys.*, 17:29753–29763.

Chan, C. K., Ha, Z. Y., and Choi, M. Y. (2000). Study of Water Activities of Aerosols of Mixtures of Sodium and Magnesium Salts. *Atmos. Environ.*, 34:4795–4803.

Chen, Y. L., DeMott, P. J., Kreidenweis, S. M., Rogers, D. C., and Sherman, D. E. (2000). Ice Formation by Sulfate and Sulfuric Acid Aerosol Particles Under Upper-Tropospheric Conditions. *J. Atmos. Sci.*, 57:3752–3766.

Cohen, M. D., Flagan, R. C., and Seinfeld, J. H. (1987a). Studies of Concentrated Electrolyte-Solutions Using the Electrodynamic Balance.1. Water Activities for Single-Electrolyte Solutions. *J. Phys. Chem.*, 91:4563–4574.

Cohen, M. D., Flagan, R. C., and Seinfeld, J. H. (1987b). Studies of Concentrated Electrolyte-Solutions Using the Electrodynamic Balance.3. Solute Nucleation. *J. Phys. Chem.*, 91:4583–4590.

Colberg, C. A., Krieger, U. K., and Peter, T. (2004). Morphological Investigations of Single Levitated H2SO4/NH3/H2O Aerosol Particles During Deliquescence/Efflorescence Experiments. *J. Phys. Chem. A*, 108:2700–2709.

Colberg, C. A., Luo, B. P., Wernli, H., and Koop, T., Peter, T. (2003). A Novel Model to Predict the Physical State of Atmospheric H2SO4/NH3/H2O Aerosol Particles. *Atmos. Chem. Phys.*, 3:909–924.

Cziczo, D. J., Nowak, J. B., Hu, J. H., and Abbatt, J. P. D. (1997). Infrared Spectroscopy of Model Tropospheric Aerosols as a Function Of Relative Humidity: Observation of Deliquescence and Crystallization. *J. Geophys. Res. Atmos.*, 102:18843–18850.

Dai, D. J., Peters, S. J., and Ewing, G. E. (1995). Water-Adsorption and Dissociation on Nacl Surfaces. *J. Phys. Chem.*, 99:10299–10304.

Davies, J. F., and Wilson, K. R. (2016). Raman Spectroscopy of Isotopic Water Diffusion in Ultraviscous, Glassy, and Gel States in Aerosol by use of Optical Tweezers. *Anal. Chem.*, 88:2361–2366.

Dette, H. P., and Koop, T. (2015). Glass Formation Processes in Mixed Inorganic/Organic Aerosol Particles. *J. Phys. Chem. A*, 119:4552–4561.

Donahue, N. M., Robinson, A. L., Stanier, C. O., and Pandis, S. N. (2006). Coupled Partitioning, Dilution, and Chemical Aging of Semivolatile Organics. *Environ. Sci. Technol.*, 40:2635–2643.

Dougle, P. G., Veefkind, J. P., and ten Brink, H. M. (1998). Crystallisation of Mixtures of Ammonium Nitrate, Ammonium Sulphate and Soot. *J. Aerosol Sci.*, 29:375–386.

Freney, E. J., Martin, S. T., and Buseck, P. R. (2009). Deliquescence and Efflorescence of Potassium Salts Relevant to Biomass-Burning Aerosol Particles. *Aerosol Sci. Technol.*, 43:799–807.

Gough, R. V., Chevrier, V. F., and Tolbert, M. A. (2014). Formation of Aqueous Solutions on Mars via Deliquescence of Chloride-Perchlorate Binary Mixtures. *Earth Planet Sci. Lett.*, 393:73–82.

Gupta, D., Eom, H. J., Cho, H. R., and Ro, C. U. (2015a). Hygroscopic Behavior of NaCl-$MgCl_2$Mixture Particles as Nascent Sea-Spray Aerosol Surrogates and Observation of Efflorescence During Humidification. *Atmos. Chem. Phys.*, 15:11273–11290.

Gupta, D., Kim, H., Park, G., Li, X., Eom, H. J., and Ro, C. U. (2015b). Hygroscopic Properties of NaCl and $NaNO_3$Mixture Particles as Reacted Inorganic Sea-Salt Aerosol Surrogates. *Atmos. Chem. Phys.*, 15:3379–3393.

Ha, Z. Y. and Chan, C. K. (1999). The Water Activities of $MgCl_2$, $Mg(NO_3)$, $MgSO_4$, and Their Mixtures. *Aerosol Sci. Technol.*, 31:154–169.

Hyslop, N. P. (2009). Impaired Visibility: The Air Pollution People See. *Atmos. Environ.*, 43:182–195.

IPCC (2013). *The Physical Science Basis. Contribution of Working Group I to the Fifth Assessment Report of the Intergovernmental Panel on Climate Change*. Cambridge, United Kingdom and New York, USA.

Kendall, T. A., and Martin, S. T. (2005). Mobile Ions on Carbonate Surfaces. *Geochim. Cosmochim. Acta*, 69:3257–3263.

Kokkola, H., Yli-Pirila, P., Vesterinen, M., Korhonen, H., Keskinen, H., Romakkaniemi, S., Hao, L., Kortelainen, A., Joutsensaari, J., Worsnop, D. R., Virtanen, A., and Lehtinen, K. E. J. (2014). The Role of Low Volatile Organics on Secondary Organic Aerosol Formation. *Atmos. Chem. Phys.*, 14:1689–1700.

Koop, T., Bookhold, J., Shiraiwa, M., and Poschl, U. (2011). Glass Transition and Phase State of Organic Compounds: Dependency on Molecular Properties and Implications for Secondary Organic Aerosols in the Atmosphere. *Phys. Chem. Chem. Phys.*, 13:19238–19255.

Kuwata, M., and Martin, S. T. (2012). Phase of Atmospheric Secondary Organic Material Affects its Reactivity. *Proc. Natl. Acad. Sci. USA*, 109:17354–17359.

Lamb, D., Moyle, A. M., and Brune, W. H. (1996). The Environmental Control of Individual Aqueous Particles in a Cubic Electrodynamic Levitation System. *Aerosol Sci. Technol.*, 24:263–278.

Lee, C. T., and Hsu, W. C. (2000). The Measurement of Liquid Water Mass Associated with Collected Hygroscopic Particles. *J. Aerosol Sci.*, 31:189–197.

Li, X., Gupta, D., Eom, H. J., Kim, H., and Ro, C. U. (2014). Deliquescence and Efflorescence Behavior of Individual NaCl and KCl Mixture Aerosol Particles. *Atmos. Environ.*, 82:36–43.

Li, Y. J., Liu, P. F., Gong, Z. H., Wang, Y., Bateman, A. P., Bergoend, C., Bertram, A. K., and Martin, S. T. (2015). Chemical Reactivity and Liquid/Nonliquid States of Secondary Organic Material. *Environ. Sci. Technol.*, 49:13264–13274.

Lightstone, J. M., Onasch, T. B., Imre, D., and Oatis, S. (2000). Deliquescence, Efflorescence, and Water Activity in Ammonium Nitrate and Mixed Ammonium Nitrate/Succinic Acid Microparticles. *J. Phys. Chem. A*, 104:9337–9346.

Liu, P., Li, Y. J., Wang, Y., Gilles, M. K., Zaveri, R. A., Bertram, A. K., and Martin, S. T. (2016). Lability of Secondary Organic Particulate Matter. *Proc. Natl. Acad. Sci. USA*, 113:12643–12648.

Liu, Y., Yang, Z., Desyaterik, Y., Gassman, P. L., Wang, H., and Laskin, A. (2008). Hygroscopic Behavior of Substrate-Deposited Particles Studied by Micro-FT-IR Spectroscopy and Complementary Methods of Particle Analysis. *Anal. Chem.*, 80:633–642.

Londahl, J., Massling, A., Pagels, J., Swietlicki, E., Vaclavik, E., and Loft, S. (2007). Size-Resolved Respiratory-Tract Deposition of

Fine and Ultrafine Hydrophobic and Hygroscopic Aerosol Particles During Rest and Exercise. *Inhal. Toxicol.*, 19:109–116.

Luna, M., Rieutord, F., Melman, N. A., Dai, Q., and Salmeron, M. (1998). Adsorption of Water on Alkali Halide Surfaces Studied by Scanning Polarization Force Microscopy. *J. Phys. Chem. A*, 102:6793–6800.

Martin, S. T. (2000). Phase Transitions of Aqueous Atmospheric Particles. *Chem. Rev.*, 100:3403–3453.

Martin, S. T., Schlenker, J. C., Malinowski, A., Hung, H. M., and Rudich, Y. (2003). Crystallization of Atmospheric Sulfate-Nitrate-Ammonium Particles. *Geophys. Res. Lett.*, 30:2102, doi:10.1029/2003gl017930.

Mifflin, A. L., Smith, M. L., and Martin, S. T. (2009). Morphology Hypothesized to Influence Aerosol Particle Deliquescence. *Phys. Chem. Chem. Phys.*, 11:10095–10107.

Nah, T., McVay, R. C., Zhang, X., Boyd, C. M., Seinfeld, J. H., and Ng, N. L. (2016). Influence of Seed Aerosol Surface Area and Oxidation Rate on Vapor Wall Deposition and SOA Mass Yields: A Case Study with α-Pinene Ozonolysis. *Atmos. Chem. Phys.*, 16:9361–9379.

Pankow, J. F. (1994). An Absorption Model of the Gas Aerosol Partitioning Involved in the Formation of Secondary Organic Aerosol. *Atmos. Environ.*, 28:189–193.

Peters, S. J., and Ewing, G. E. (1997). Thin Film Water on NaCl (100) Under Ambient Conditions: An Infrared Study. *Langmuir*, 13:6345–6348.

Poschl, U. (2005). Atmospheric Aerosols: Composition, Transformation, Climate and Health Effects. *Angew. Chem. Int. Ed.*, 44:7520–7540.

Richardson, C. B., and Snyder, T. D. (1994). A study of Heterogeneous Nucleation in Aqueous-Solutions. *Langmuir*, 10:2462–2465.

Romakkaniemi, S., Hämeri, K., Väkevä, M., and Laaksonen, A. (2001). Adsorption of Water on 8−15 nm NaCl and $(NH_4)_2SO_4$ Aerosols Measured Using an Ultrafine Tandem Differential Mobility Analyzer. *J. Phys. Chem. A*, 105: 8183–8188.

Rosenoern, T., Schlenker, J. C., and Martin, S. T. (2008). Hygroscopic Growth of Multicomponent Aerosol Particles Influenced by Several Cycles Of Relative Humidity. *J. Phys. Chem. A*, 112:2378–2385.

Schindelholz, E., Tsui, L. K., and Kelly, R. G. (2014). Hygroscopic Particle Behavior Studied by Interdigitated Array Microelectrode Impedance Sensors. *J. Phys. Chem. A*, 118:167–177.

Schlenker, J. C., Malinowski, A., Martin, S. T., Hung, H. M., and Rudich, Y. (2004). Crystals Formed at 293 K by Aqueous Sulfate-Nitrate-Ammonium-Proton Aerosol Particles. *J. Phys. Chem. A*, 108:9375–9383.

Shiraiwa, M., Pfrang, C., Koop, T., and Poschl, U. (2012). Kinetic Multi-Layer Model of Gas-Particle Interactions in Aerosols and Clouds (KM-GAP): Linking Condensation, Evaporation and Chemical Reactions of Organics, Oxidants and Water. *Atmos. Chem. Phys.*, 12:2777–2794.

Shiraiwa, M., Pfrang, C., and Poschl, U. (2010). Kinetic Multi-Layer Model of Aerosol Surface and Bulk Chemistry (KM-SUB): The Influence of Interfacial Transport and Bulk Diffusion on the Oxidation of Oleic Acid by Ozone. *Atmos. Chem. Phys.*, 10:3673–3691.

Smith, M. L., Kuwata, M., and Martin, S. T. (2011). Secondary Organic Material Produced by the Dark Ozonolysis of Alpha-Pinene Minimally Affects the Deliquescence and Efflorescence of Ammonium Sulfate. *Aerosol Sci. Technol.*, 45:244–261.

Tang, I. N. (1996). Chemical and Size Effects of Hygroscopic Aerosols on Light Scattering Coefficients. *J. Geophys. Res. Atmos.*, 101:19245–19250.

Tang, I. N., and Munkelwitz, H. R. (1994). Water Activities, Densities, and Refractive-Indexes of Aqueous Sulfates and Sodium-Nitrate Droplets of Atmospheric Importance. *J. Geophys. Res. Atmos.*, 99:18801–18808.

Varutbangkul, V., Brechtel, F. J., Bahreini, R., Ng, N. L., Keywood, M. D., Kroll, J. H., Flagan, R. C., Seinfeld, J. H., Lee, A., and Goldstein, A. H. (2006). Hygroscopicity of Secondary Organic Aerosols Formed by Oxidation of Cycloalkenes, Monoterpenes, Sesquiterpenes, and Related Compounds. *Atmos. Chem. Phys.*, 6:2367–2388.

Virtanen, A., Joutsensaari, J., Koop, T., Kannosto, J., Yli-Pirila, P., Leskinen, J., Makela, J. M., Holopainen, J. K., Poschl, U., Kulmala, M., Worsnop, D. R., and Laaksonen, A. (2010). An Amorphous Solid State of Biogenic Secondary Organic Aerosol Particles. *Nature*, 467:824–827.

Wang, B. B., O'Brien, R. E., Kelly, S. T., Shilling, J. E., Moffet, R. C., Gilles, M. K., and Laskin, A. (2015). Reactivity of Liquid and Semisolid Secondary Organic Carbon with Chloride and Nitrate in Atmospheric Aerosols. *J. Phys. Chem. A*, 119:4498–4508.

Wang, F., Zhang, Y. H., Li, S. H., Wang, L. Y., and Zhao, L. J. (2005). A Strategy for Single Supersaturated Droplet Analysis: Confocal Raman Investigations on the Complicated Hygroscopic Properties of Individual $MgSO_4$Droplets on the Quartz Substrate. *Anal. Chem.*, 77:7148–7155.

Wong, J. P. S., Lee, A. K. Y., and Abbatt, J. P. D. (2015). Impacts of Sulfate Seed Acidity and Water Content on Isoprene Secondary Organic Aerosol Formation. *Environ. Sci. Technol.*, 49:13215–13221.

Zhang, X., Mcvay, R. C., Huang, D. D., Dalleska, N. F., Aumont, B., Flagan, R. C., and Seinfeld, J. H. (2015). Formation and Evolution of Molecular Products in Alpha-Pinene Secondary Organic Aerosol. *Proc. Natl. Acad. Sci. USA*, 112:14168–14173.

Zhao, L. J., Zhang, Y. H., Wei, Z. F., Cheng, H., and Li, X. H. (2006). Magnesium Sulfate Aerosols Studied by FTIR Spectroscopy: Hygroscopic Properties, Supersaturated Structures, and Implications for Seawater Aerosols. *J. Phys. Chem. A*, 110:951–958.

Zieger, P., Aalto, P. P., Aaltonen, V., Aijala, M., Backman, J., Hong, J., Komppula, M., Krejci, R., Laborde, M., Lampilahti, J., de Leeuw, G., Pfuller, A., Rosati, B., Tesche, M., Tunved, P., Vaananen, R., Petaja, T. (2015). Low Hygroscopic Scattering Enhancement of Boreal Aerosol and the Implications for a Columnar Optical Closure Study. *Atmos. Chem. Phys.*, 15:7247–7267.

Zobrist, B., Marcolli, C., Pedernera, D. A., and Koop, T. (2008). Do Atmospheric Aerosols form Glasses? Atmos. *Chem. Phys.*, 8:5221–5244.